Available online at www.sciencedirect.com
SCIENCE DIRECT®
Journal of Organometallic Chemistry 689 (2004) 3287–3300
Journal of Organometallic Chemistry
www.elsevier.com/locate/jorganchem

A higher yielding route to octasilsesquioxane cages using tetrabutylammonium fluoride, Part 2: further synthetic advances, mechanistic investigations and X-ray crystal structure studies into the factors that determine cage geometry in the solid state

Alan R. Bassindale [a,*], Huiping Chen [b], Zhihua Liu [a], Iain A. MacKinnon [c], David J. Parker [a], Peter G. Taylor [a,*], Yuxing Yang [a], Mark E. Light [d], Peter N. Horton [d], Michael B. Hursthouse [d]

[a] *Department of Chemistry, Open University, Walton Hall, Milton Keynes, MK7 6AA, UK*
[b] *Dow Corning Corporation, Midland, MI 48686, USA*
[c] *Dow Corning Ltd., Barry, CF63 2YL, UK*
[d] *EPSRC National Crystallography Service, University of Southampton, Highfield, Southampton, SO17 1BJ, UK*

Received 26 January 2004; accepted 25 June 2004
Available online 28 August 2004

Abstract

The recently-reported reaction of triethoxysilanes with tetrabutylammonium fluoride in the presence of scarce water provides a higher yielding route to substituted octasilsesquioxane cages. Further cages have now been prepared in good yield using this route and their X-ray crystal structures demonstrate that their cage geometries in the solid state are very similar with the packing constraints of the crystal lattices appearing to have the greatest influence on the geometry of the cage core. The mechanism of the reaction has been examined and the proposed mechanism of cage formation validated, though its exclusivity has not been categorically proven. By careful choice of reaction conditions, dramatic increases in rate and yield have been demonstrated.

Keywords: T8 silsequioxane cage; Alkoxysilane; X-ray study; Mechanism

1. Introduction

T_8 spherosilicate silsesquioxane cages, and in particular octahydro-octasilsesquioxane **1**, have been used extensively as scaffolds for the development of liquid crystals [1,2], biocompatible materials [3], catalysts [4,5] and dendrimers [6]. The notation T_8 denotes that the closed cage comprises eight T-silicon atoms (i.e., silicon atoms bonded to three oxygens).

Initial routes to functionalised T_8 cages focussed on the hydrosilylation of **1** [6] but were limited by the poor yields of the starting cage prepared from the hydrolysis of trichlorosilane [7,8]. Other routes involving the controlled hydrolysis of trichloro- or trialkoxysilanes [9–11] or acid catalysed hydrolysis of 3-aminopropyltriethoxysilane [6], allowing functionalised cages to be constructed in a single synthetic step, have also been reported but similarly suffer from yields of no more than 30% (Scheme 1).

We have recently published a higher yielding route to T_8 cages using trialkoxysilanes, catalysed by tetrabutylammonium fluoride (TBAF), for a series of functionalised T_8's and reported improved yields of up to 95%

* Corresponding authors. Tel.: +44 1908 652512; fax: +44 1908 858327.
E-mail address: p.g.taylor@open.ac.uk (P.G. Taylor).

0022-328X/$ - see front matter © 2004 Elsevier B.V. All rights reserved.
doi:10.1016/j.jorganchem.2004.06.063

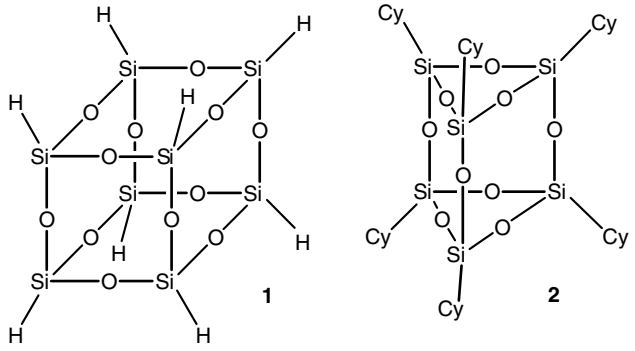

Scheme 1.

[12]. We suggested that because our source of TBAF contained 5% water, complexation of the basic fluoride ion to water enabled hydroxide ion to attack the alkoxysilane to form the corresponding silanol. Further interaction of fluoride ion with the hydrogen of this silanol would similarly lead to an increase in the nucleophilicity of the oxygen leading to further reaction and Si–O–Si bond formation. We have also proposed that such a mechanism is present in the ring expansion reactions of hexacyclohexyl-hexasilsesquioxane **2** by dialkyl/aryl diethoxysilanes in the presence of scarce water and TBAF that leads to isolable and fully characterised T_6D_1 **3** and T_6D_2 cages (for example regioisomer **4**) [13] (Scheme 2).

In this paper we examine further functionalised T_8 cages made using our scarce water, TBAF catalysed route and consider in more detail the structural and geometric implications of different pendant functionalities attached to the cage's Si_8O_{12} core. We also further probe the mechanism of cage formation.

2. Results and discussion

Following our previously reported synthesis of T_8 cages with 'wet' TBAF we have prepared a number of new cages in a similar way with respectable yields. The reaction of 3-*para*-methoxyphenylpropyltriethoxysilane with TBAF in chloroform for 24 h gave the corresponding pure octa-3-*para*-methoxyphenylpropyl-octasilsesquioxane **5** in 17% yield as the only isolated cage compound and with no further purification or chromatographic separation of components required. *Iso*-octyltrimethoxysilane was similarly reacted with TBAF in a dichloromethane solution to give octa-*iso*-octyl-octasilsesquioxane **6** as the major component which could be purified by column chromatography with an isolated yield of 43% (Scheme 3).

In order to probe further our proposed mechanism of cage formation [12] we have conducted a series of experiments on the reactions of cyclopentyltriethoxysilane or cyclohexyltriethoxysilane with TBAF to give the corresponding T_8 cages **7** or **8**, respectively. By preparing **7** firstly using stock TBAF solution containing ≈5% water and then using two TBAF solutions containing different proportions of ^{18}O and ^{16}O-labelled water, we have been able to use a Fourier transform ion cyclotron resonance mass spectrometer (FTICR-MS) to look at how the mean mass of a selected cage-comprising ion changes from experiment to experiment. This has allowed us to see whether ^{18}O is incorporated into the cage from the water, determine an average number of ^{18}O atoms per cage and see how that number changes with ^{18}O content in the water. As discussed later, we were unable to determine the exact proportion of ^{18}O-labelled water in our stock solutions and thus comparisons with the proportion of ^{18}O in the sislesquioxane cages is qualitative rather than quantitative.

Fig. 1 shows the FTICR mass spectrum of the $[M + NH_4]^+$ ion of **7** prepared (a) in the absence of ^{18}O-labelled water in the TBAF solution, (b) with a low proportion of ^{18}O-labelled water-containing TBAF solution and (c) with a higher proportion of ^{18}O-labelled water-containing TBAF solution. Our stock supply of TBAF was a THF solution containing 5% water and was used to conduct reaction (a). Reaction (b) was performed similarly but using a solution of TBAF which

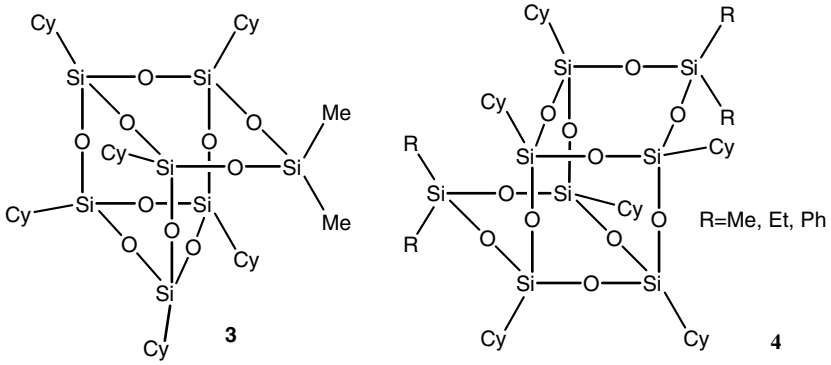

Scheme 2.

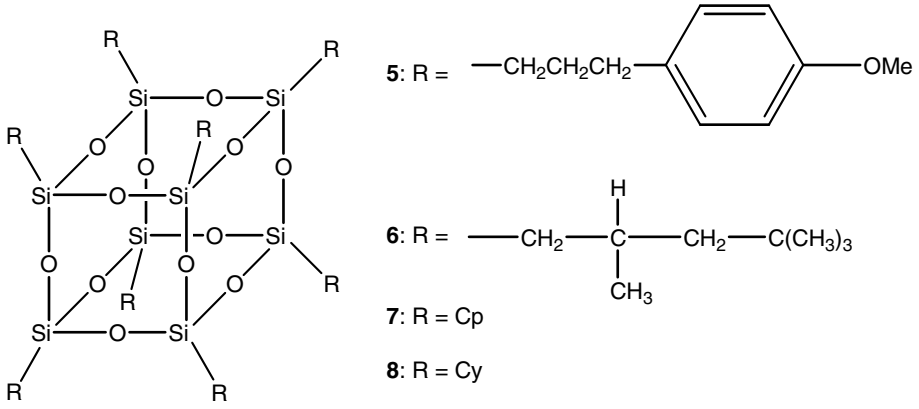

Scheme 3.

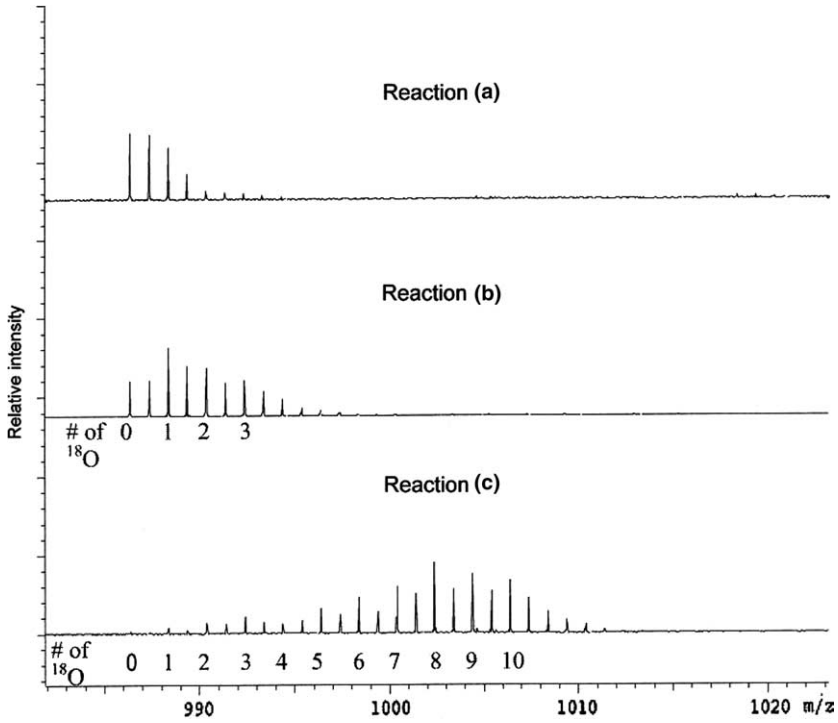

Fig. 1. FTICR mass spectra of the $[M + NH_4]^+$ ion of **7** prepared from TBAF solutions containing (a) no ^{18}O-labelled water, (b) a low proportion of ^{18}O-labelled water and (c) a higher proportion of ^{18}O-labelled water-containing TBAF solution.

had been dried over molecular sieves to remove most of its water content. Removing all the moisture was not a practical possibility because of the strong hydrogen bonding by fluoride ion. ^{18}O enriched water was then added to make the final water content 5%. Reaction (c) used a similar portion of pre-dried batch TBAF solution but the added water had a higher ^{18}O-label enrichment.

The isotope pattern for the $[M + NH_4]^+$ ion of reaction (a) is relatively simple as expected with no incorporation of ^{18}O isotope, however for (b) there is greater complexity and a slightly higher mean mass for the pseudomolecular ion due to the incorporation of up to three ^{18}O atoms into the cage. In reaction (c) the isotopic distribution is even more complex with a higher mean mass for the $[M + NH_4]^+$ ion. This demonstrates that the extent of ^{18}O atom incorporation is more extensive in the products of reaction (c) than in reaction (b) and is consistent with the higher proportion of ^{18}O labelled water present at the start of reaction (c).

The extent of ^{18}O atom incorporation can be quantified in terms of the average number of ^{18}O atoms per cage (A_{O18}) from the isotopic distribution of a given pseudomolecular ion of T_8 using the following expression:

$$A_{O18} = (M_{meas} - M_{O16})/(m_{O18} - m_{O16}).$$

M_{meas}, M_{O16}, m_{O18} and m_{O16} are the average mass measured for the pseudomolecular ion of a T_8 cage containing both ^{18}O and ^{16}O isotopes, the average mass measured for the pseudomolecular ion of a T_8 cage containing all (i.e., 12) ^{16}O's, the mass of an ^{18}O atom, and the mass of an ^{16}O atom, respectively. M_{meas} and M_{O16} are mathematically derived by calculating each isotopic peak's fractional intensity contribution to the overall intensity, multiplying that fraction by its mass and then summing the results. The values of M_{meas} and A_{O18} for reactions (a), (b) and (c) are given in Table 1. The value of A_{O18} obtained is shown to be dependent on the amount of ^{18}O present in the water.

A similar statistical treatment of the FTICR-MS data was carried out on samples of **7** and **8** prepared under identical reaction conditions using fractions of the same TBAF solution containing ^{18}O-labelled water (reactions (e) and (g), respectively) as was used to conduct reaction (c). Values of A_{O18} based on both the $[M + H]^+$ and $[M + NH_4]^+$ ions were calculated and compared to samples of **7** and **8** prepared without labelled water (reactions (d) and (f), respectively) as shown in Table 2.

Confirmation that the statistical analysis results are reproducible and independent of which pseudomolecular ion is chosen, is provided by the mean A_{O18} values calculated from the isotopic distributions of the $[RT_8 + NH_4]^+$ and $[RT_8 + H]^+$ ions which are, within experimental error, the same as each other. Also, as reaction (e) is effectively a repeat of reaction (c) we find as expected that their A_{O18} values are essentially the same as each other within experimental error. The variation that we do see between these experiments we presume reflects the different reaction times we employed and the hygroscopic nature of our TBAF solution. The very similar A_{O18} values of the different cages prepared in reactions (e) and (g) plus the observation that ^{18}O inclusion in the cage is proportional to the ^{18}O content of the water in Table 1 together compliment our proposed reaction mechanism whereby the oxygens that form the cage structure are derived from the water of the TBAF and not from the alkoxy-groups of the starting silane.

Our investigations to determine accurately the proportion of ^{18}O in our starting TBAF solutions by studying the hydrolysis of monochlorosilanes (chlorotrimethylsilane and chloromethyldiphenylsilane) to their corresponding disiloxanes with ^{18}O-labelled water were inconclusive despite the water in the TBAF solutions being the only oxygen atom source available for the reactions. The $^{18}O/^{16}O$ ratio of the disiloxanes prepared from the same TBAF solution that was used in reaction (c) were calculated from the EI mass spectral data from GC–MS analyses. The theoretical A_{O18} values for the octasilsesquioxane cages was then determined from these ratios. Corresponding A_{O18} values ranging from 7.7 to 8.5 were obtained and were found to vary from day to day and sample to sample. This means that though the corresponding A_{O18} values calculated for the disiloxane reactions are similar to that measured for the T_8 cage in reaction (c), the $^{18}O/^{16}O$ ratios measured in the disiloxanes are not accurate representations of the $^{18}O/^{16}O$ ratio in the water content of the TBAF solution.

We attribute the reason why the A_{O18} values for the disiloxanes were consistently higher than that calculated for the cage in reaction (c) to the fact that the disiloxane reactions were performed first and the hygroscopic nature of our TBAF solutions may have resulted in a decrease in the $^{18}O/^{16}O$ ratio between experiments. Our findings bring us to conclude that while oxygen incorporation into T_8 cages from the ethoxy-groups of the triethoxysilane cannot be ruled out, this mechanism requires the fluoride ion promoted breaking of an O–C_{sp^3} bond under mild conditions. These limitations make such an alternative mechanism less plausible and point to our fluoride/water mechanism as being far more probable. Our attempts to prepare **7** by replacing TBAF with tetrabutylammonium chloride were unsuccessful and only starting materials were retrieved from the reaction over similar time scales. This points to fluoride ion as having a critical role in the mechanism of cage formation.

Table 1
Values of M_{meas} and A_{O18} calculated for **7** in reactions (a), (b) and (c) from the corresponding isotopic distribution of the $[M + NH_4]^+$ ion shown in Fig. 1

Reaction	M_{meas} ($[CyPT_8 + NH_4]^+$ ions)	A_{O18}
(a)	988.0612[a]	0
(b)	990.1377	1.0
(c)	1001.7673	6.8

[a] $M_{meas} = M_{O16}$.

Table 2
Values of M_{meas} and A_{O18} calculated for **7** or **8** in reactions (d), (e), (f) and (g) from the isotopic distributions of the $[M + H]^+$ and $[M + NH_4]^+$ ions observed by FTICR-MS

Reaction	Compound	R	M_{meas} for $[RT_8 + H]^+$ ions	Mean number of ^{18}O from $[RT_8 + H]^+$ ions	M_{meas} for $[RT_8 + NH_4]^+$ ions	Mean number of ^{18}O from $[RT_8 + NH_4]^+$ ions	A_{O18}
(d)	**7**	CyP	970.4385	0	987.6062	0	0
(e)	**7**	CyP	983.1270	6.3	1000.2182	6.3	6.3
(f)	**8**	CyH	1082.7616	0	1099.8050	0	0
(g)	**8**	CyH	1095.9170	6.6	1112.6543	6.4	6.5

Table 3
The isolated yield of **7** obtained from reactions of cyclopentyltriethoxysilane with TBAF in different solvents

Solvent	Reaction time (h)	Yield of T_8 (%)
Chloroform	48	13
THF	12	23
Acetone	4	95

Table 3 shows the effect of different solvents on the yield and reaction times for the preparation of **7** using the same TBAF solution. The low solubility of **7** in many organic solvents, particularly acetone, may explain why it is formed in such a high yield since it precipitates readily from solution upon formation and therefore drives the reaction towards completion.

The synthesis of **7** has also been studied using NMR spectroscopy where the TBAF solution contained different levels of moisture. Under dried conditions the formation of the pentacoordinate species $[NBu_4]^+$ $[cyclopentylSiF_4]^-$ **9** was observed in the ^{29}Si NMR spectrum of the reaction mixture as a pentet at −113.99 ppm alongside that of **7** at −66.55 ppm. The formation of **9** is consistent with cage formation taking place using the remaining trace water in the TBAF until its supply is exhausted and then fluoride ion directly attacks the remaining cyclopentyltriethoxysilane (Fig. 2). Under conditions of excess water the ^{29}Si NMR spectra of the reaction mixture showed no pentacoordinate species but a mixture containing a reduced amount of **7** and an array of silanol-containing partial cage structures. This observation underlines the importance of careful control of the TBAF's water content in order to obtain the highest yield of cage product.

To understand the role of these partial cage structures as potential intermediates in cage synthesis we used ^{29}Si NMR to study the formation of **7** with time in a deuteriochloroform solution containing TBAF. Deuteriochloroform was chosen as it is a relatively good solvent for solublising **7**. After stirring a 2:1 ratio solution of cyclopentyltriethoxysilane and TBAF for 24 h the ^{29}Si NMR spectrum of the reaction mixture showed a sharp peak determined from standard samples to arise from **7** and an unresolved array of smaller sharp peaks between −60 and −70 ppm. The peaks in the −60 to −64 ppm region particularly suggested the presence of silanol groups in partial cages. After a further 24 h the peak for **7** had grown in relation to others and precipitation from acetone afforded **7** in 13% yield.

To test whether these uncharacterised silanol-containing species were formed from the breakdown of **7** and so were end products in their own right or whether they were intermediates in the formation of **7** we undertook the synthesis of **7** in deuteriochloroform with a twofold excess of TBAF to cyclopentyltriethoxysilane. After 24 h the ^{29}Si NMR spectrum showed only a quintet at −113.99 ppm corresponding to **9** and a single peak at −66.55 ppm for **7**. By stopping and working-up the reaction, **7** was isolated with an improved yield of 23%, consistent with the greater conversion of the silanol-containing partial cages into **7** by the excess of fluoride ion and their consequent absence from the ^{29}Si NMR spectrum. If these silanol-containing compounds were formed from the breakdown of **7** then the yield of **7** would have been expected to be less due to the excess of fluoride ion promoting more extensive cage breakdown and consequently increasing the proportion of silanol-containing partial cage compounds (Scheme 4).

We have also studied the X-ray crystal structures of many of the octasilsesquioxane cages we have synthesised and have recently reported the structures of **7**, **14** and **15** [12]. This paper supplements these with new or further structures for **5**, **8** and **10**.

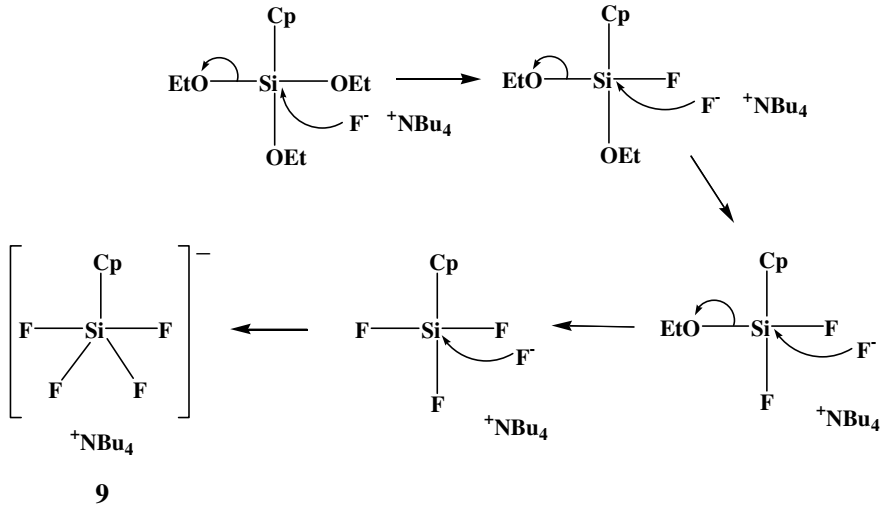

Fig. 2. The proposed mechanism for the formation of 9 from cyclopentyltriethoxysilane and TBAF in the absence of water.

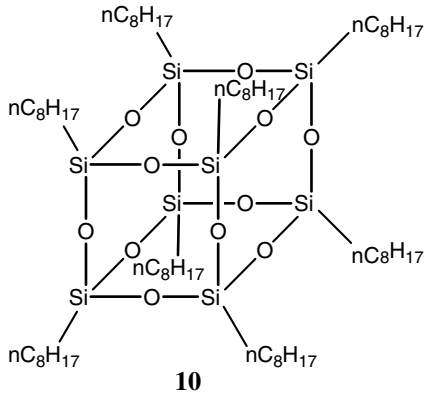

Scheme 4.

Figs. 3 and 4 show how the octyl arms of **10** and to a lesser extent the 3-*para*-methoxyphenylpropyl arms of **5** align themselves along one axis. Fig. 5 additionally shows that the octyl arms of **10** do not interdigitate with those of adjacent molecules in the lattice. This arrangement of arms is strongly reminiscent of the phase aligning of mesogenic arms in liquid crystal silsesquioxane cages proposed by Maurer et al. [14] and supporting the work of Goodby and Mehl [15] on the liquid crystalline properties of the species formed by coupling of the cyanobiphenyl mesogen **11** with various siloxanes or **1** [15–17] Fig. 6 (Scheme 5).

Though a crystal structure for **8** was first obtained by Barry et al. [18] we have obtained three further structures which vary in both unit cell dimensions and space group. These structures **8a**, **8b** and **8c** were obtained as the crystallised products of rearrangement reactions of **2** in the presence of various alkylethoxysilanes and TBAF. While the full discussion of these rearrangements will be the subject of a future paper, their key crystal and cage dimensional data are summarised in Table 4 together with the corresponding data of selected octasilsesquioxanes from

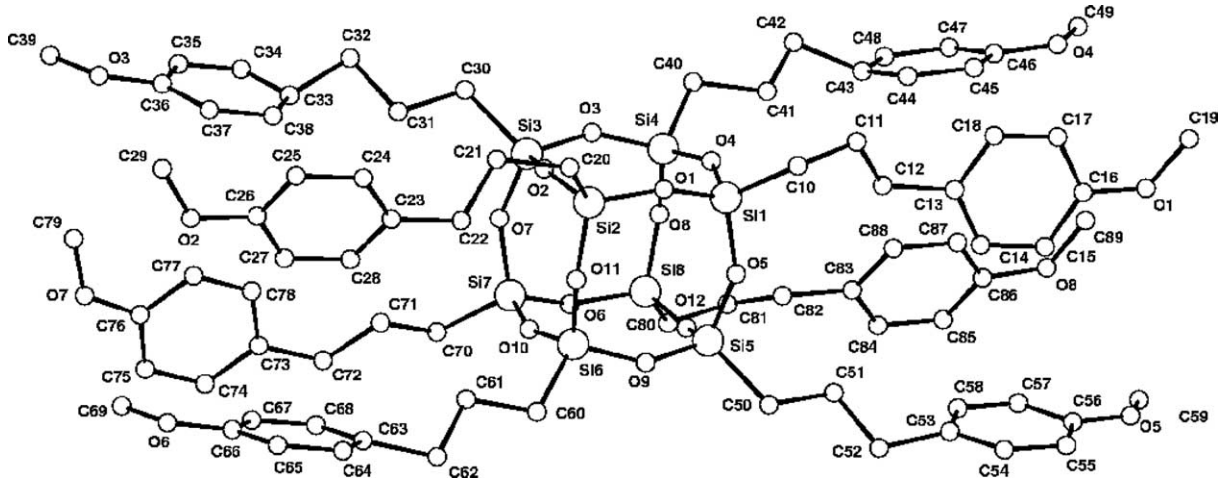

Fig. 3. The isotropic crystal structure of **5**. All eight arms are disordered over two positions (50/50 ratio) with only one orientation being shown here. Arm orientations alternate between adjacent unit cells. Hydrogen atoms are omitted for clarity.

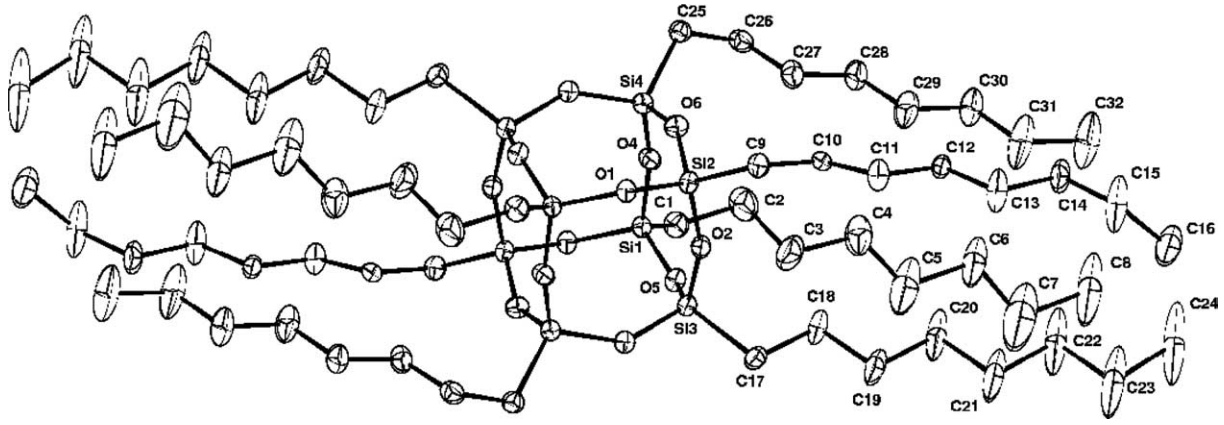

Fig. 4. ORTEP-representation of **10** with envelopes drawn at the 30% probability level. The arm beginning C9 is disordered over two positions (60/40 ratio) but only the major orientation is shown here. The hydrogen atoms are omitted for clarity.

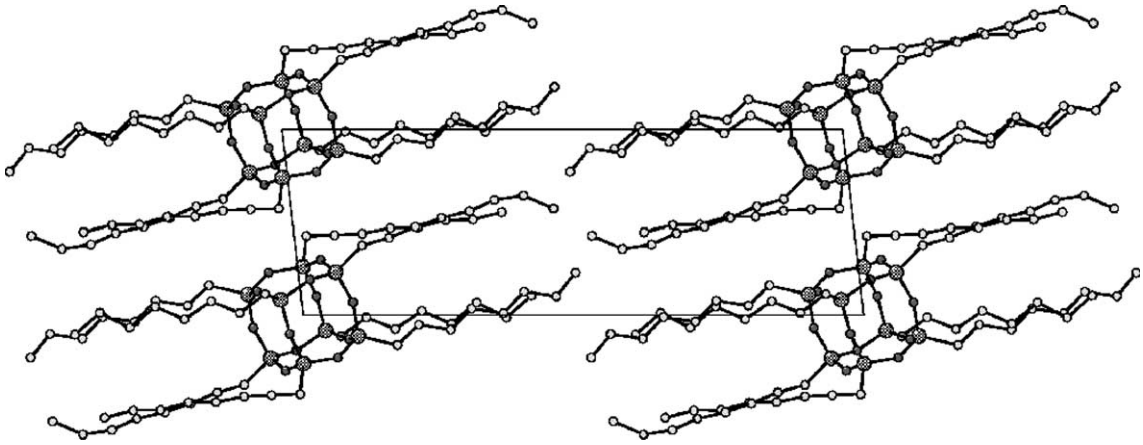

Fig. 5. Isotropic structure view down the *b* axis of the unit cell of **10** showing the packing arrangement of the molecules. The hydrogen atoms are not shown for clarity.

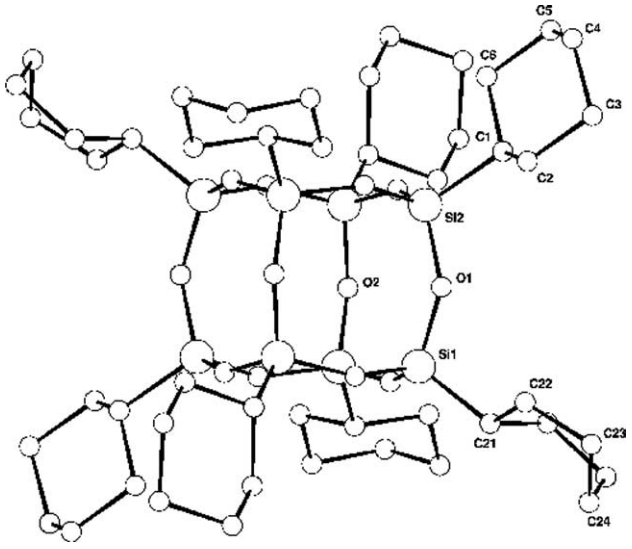

Fig. 6. The isotropic crystal structure **8a**. The rings in the *boat* conformation are disordered over three positions (only one orientation is shown here) around the −3 axis in a manner that only boat conformations can exist. Hydrogen atoms omitted for clarity.

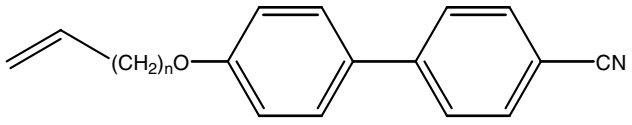

n =2, 4 or 9 **11**

Scheme 5.

the literature. Structure **8b** contains three independent molecules **8b.1**, **8b.2** and **8b.3** each of which is shown in Fig. 7.

Close inspection of the cyclohexyl rings of **8a** and **8b** shows that the constraint of crystal packing sometimes causes them to adopt a *boat* conformation. Though the often poor internal order of these crystals made obtaining high quality X-ray data difficult and resulted in larger than ideal thermal parameters we can still reasonably conclude from our data that at least a percentage of the molecules in the crystals **8a** and **8b** contain cyclohexyl rings in a real *boat* conformation, occurring in the positions suggested Figs. 8 and 9.

Table 4 shows that despite the wide variety and size of carbon-bond pendant groups considered, the variation in cage geometry is surprisingly limited given the known flexibility of the Si–O–Si and O–Si–O unit and the variation in hybridisation state and electronic environment of the binding carbon atom. While the variation in mean *ortho*, *meta* and *para* inter-silicon distances are closely linked and changes to the mean Si–O–Si and O–Si–O bond angles are also strongly related, there is little overall correspondence between them.

In particular the mean ΣO–Si–O bond angles of structures **8a**, **8b** and **8c** are different enough to span over half the total range of values observed. It is hard therefore to explain the relatively large structural differences between them by an argument based either on electronic or steric control of the geometry of the Si_8O_{12} cage core by the pendant group. Our observations are comparable with the conclusions of a similar crystal structure study of octasilsesquioxanes by Podberezskaya et al. [25]. We postulate therefore that the primary influencing factor on cage geometry in the solid state is the molecule's crystal lattice and that the influence of a carbon-bound pendant group on the geometry of a silicon to which it is attached is relatively unpronounced. This conclusion contrasts with the important influence we believe the steric bulk of a pendant group has in determining which size silsesquioxane cages are preferentially formed [12].

We are currently examining other high-yielding synthetic routes to substituted T_6, T_8, T_{10} and T_{12} silsesquioxane cages including studies of their interconversion and of their liquid crystalline and other material properties.

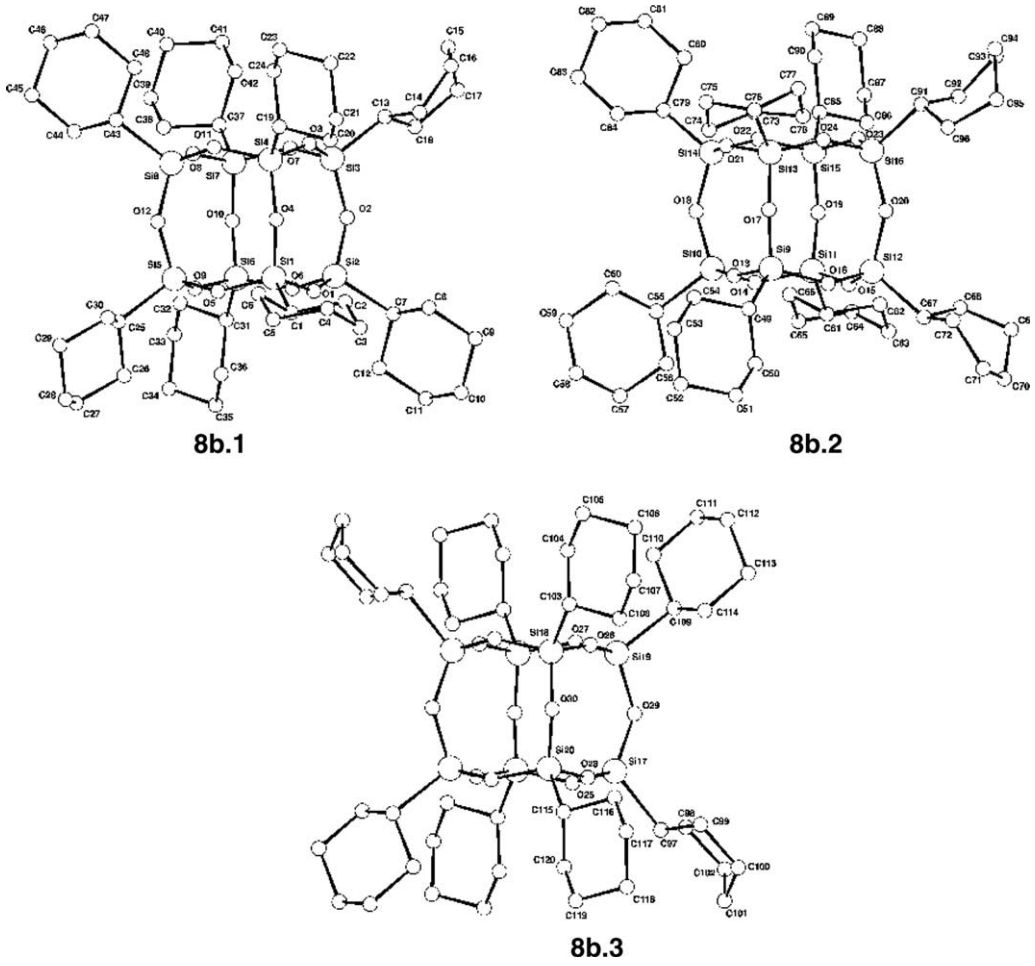

Fig. 7. The isotropic crystal structures of the three independent molecules **8b.1**, **8b.2** and **8b.3** in the asymmetric unit that comprise structure **8b**. While there is disorder in a number of the cyclohexyl rings in each molecule (only one orientation of each is shown here) the *boat* conformation does occur as shown in at least a percentage of the molecules in the crystals. The hydrogen atoms omitted for clarity.

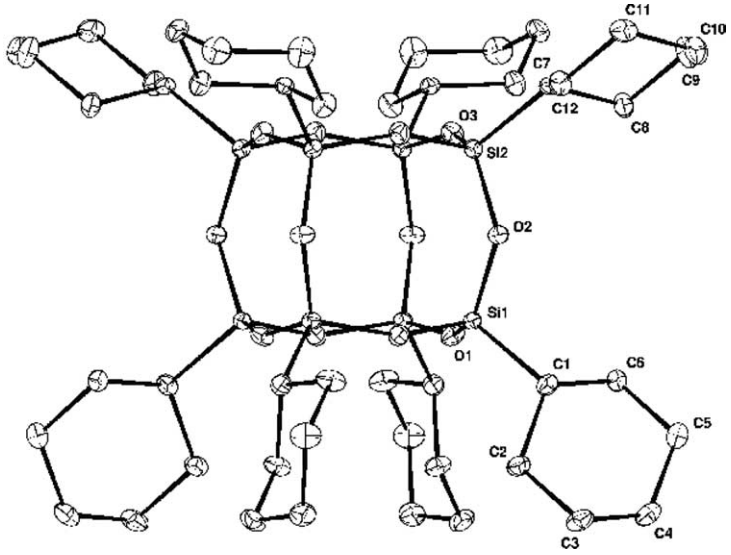

Fig. 8. ORTEP-representation of **8c** with envelopes drawn at the 30% probability level. The hydrogen atoms are omitted for clarity.

Table 4
A summary of key cage dimensional data of various substituted octasilsesquioxanes determined from the X-ray crystal structures of our own compounds and analogues the literature

Pendant group	Number	Reference	Mean Si–O (Å)	Mean Si–O–Si (°)	Mean O–Si–O (°)	Mean ΣO–Si–O (°)	*Ortho* Si–Si (**A**) (Å)	*Meta* Si–Si (**B**) (Å)	*Para* Si–Si (**C**) (Å)
Allyl	**11**	[19]	1.62	150.7	108.2	324.7	3.13	4.43	5.42
$CH_2CH_2Si(CH{=}CH_2)_3$	**12**	[20]	1.60	150.3	108.4	325.3	3.10	4.38	5.37
Vinyl	**13**	[21]	1.61	150.3	108.5	325.6	3.10	4.39	5.37
Cyclohexyl (1)	**8a**	–	1.61	150.1	108.6	325.7	3.10	4.39	5.38
i-Butyl	**14**	[21]	1.62	149.8	108.7	326.1	3.12	4.41	5.40
p-Methoxyphenylpropyl	**5**	–	1.62	149.5	108.8	326.4	3.12	4.41	5.40
Cyclohexyl (2)[a]	**8b**	–	1.61	149.4	108.8	326.4	3.11	4.39	5.38
$CH_2CH_2CMe_2CO_2Me$	**15**	[12]	1.62	149.2	108.8	326.5	3.12	4.41	5.40
n-Octyl	**10**	–	1.62	149.2	108.8	326.5	3.12	4.41	5.40
Me-piperidone	**16**	[22]	1.61	148.8	108.9	326.6	3.11	4.40	5.38
Cyclopentyl	**7**	[12]	1.62	148.6	108.9	326.8	3.12	4.41	5.40
3-Iodopropyl	**17**	[23]	1.62	149.3	109.0	326.9	3.11	4.40	5.39
Cyclohexyl (3)	**8c**	–	1.62	149.3	109.0	327.0	3.12	4.41	5.40
Benzyl[a]	**18**	[24]	1.62	148.9	109.0	327.1	3.11	4.40	5.39
Ethyl	**19**	[25]	1.61	149.3	109.0	327.1	3.10	4.39	5.37
Ph (w. acetone solvate)	**20**	[26]	1.61	149.2	109.1	327.2	3.10	4.39	5.38

[a] Average values from two or more independent molecules in the crystal.

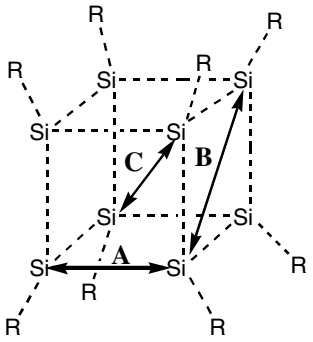

Fig. 9. A schematic outline of an octasilsesquioxane cage to show the three internal Si–Si cage distances measured. The mean values of each in the X-ray crystal structures of various examples are reported in Table 4.

3. Conclusions

The scarce-water reaction of tetrabutylammonium fluoride with substituted triethoxysilanes has been shown to be a higher yielding route to octasilsesquioxane cages. We have prepared further T_8 cages using this route and demonstrated by the comparison of the X-ray crystal structures of our cages with those in the literature that the geometry of the cages in the solid state are very similar and what differences there are between them is primarily the result of packing constraints of the crystal lattices on whole molecules rather than the influence of pendant groups on the individual cages to which they are attached.

Our investigations into the mechanism of cage formation showed that it can occur by incorporation of the oxygen atoms from the water contained in the TBAF solution and that by optimising the water's concentration improved yields of T_8 cages can be obtained. We have also shown that fluoride ion is a critical component of the reactions mechanism and that strong donor solvents such as acetone dramatically improve the reaction rate and therefore the isolated yield of T_8 cages. Our findings provide considerable supporting evidence for the mechanism of cage formation that we have previously proposed.

4. Experimental

4.1. General

IR. Infrared spectra were obtained as Nujol mulls using sodium chloride plates with a Nicolet 205 FT-IR spectrometer.

NMR. All NMR spectra were obtained using either a JEOL EX 400 NMR or a JEOL Lambda 300 NMR spectrometer with the pulse delay for ^{29}Si NMR spectra standardised at 20 s. All spectra were recorded at room temperature (25 °C) using deuterated chloroform ($CDCl_3$) dried over 4 Å molecular sieves as solvent unless stated otherwise. The NMR external reference compound was tetramethylsilane (TMS) for ^1H, ^{13}C and ^{29}Si NMR spectra. The spectral data point position of this compound was accurately located before data acquisition. ^1H–^1H and ^1H–^{13}C COSY and DEPT programs were frequently used to help the assigning of ^1H and ^{13}C NMR spectra.

GC–MS. GC–MS analyses were performed using an Agilent 5973 series instrument with a 30 m × 0.25 mm × 0.25 μm Rtx-1 column connected to the liquid injection port and a 30 m × 0.25 mm × 0.50 μm Rtx-1 column connected to the head space injection port. Conventional 70 eV electron impact (EI) ionisation was used for structural identification.

FTICR-MS. All experiments were performed on a Bruker Apex II FTICR-MS equipped with a 4.7 T

superconducting magnet and an external Analytica electrospray ionisation (ESI) source. A Cole–Parmer series 74900 syringe pump was used to continuously infuse samples into the ESI source. The instrument was operated in the positive-ion mode and data was acquired in the broadband mode.

4.2. Preparation of TBAF solutions

The TBAF came from Aldrich Chemical Company Ltd. as a 1 M THF solution and contained ≈5% water. From this a series of 'standard' solutions were prepared in THF for use in our experiments:

Solution A. The TBAF solution as purchased.

Solution B. A sample of Solution A was dried for 48 h over type 4 Å molecular sieves pre-dried for 5 days at 300 °C.

Solution C. To a sample of Solution B was added ^{18}O enriched water so as to make its content 5%.

Solution D. To a sample of Solution B was added ^{18}O enriched water so as to make its content 20%.

Solution E. To a sample of Solution A was added a 20-fold excess of water.

4.3. Synthesis of octasilsesquioxane cages using TBAF

4.3.1. 3-para-Methoxyphenylpropyltriethoxysilane

Ethanol (2.59 g, 56.4 mmol) and triethylamine (5.7 g, 56.4 mmol) were dissolved in THF (100 ml), and a solution of 3-*para*-methoxyphenylpropyltrichlorosilane (5 g, 17.6 mmol) in THF (100 ml) added to the mixture very slowly. After 1 h stirring, a white solid precipitated out. The mixture was filtered by vacuum and the filtrate collected. A yellow liquid was obtained after removal of solvent and was used at the next stage without further purification. Yield: 4.74 g (86.0%); ν_{max} (Neat/cm^{-1}) 2983, 2931, 2886, 2842, 2768, 2723, 1610, 1573, 1513, 1461, 1432, 1387, 1298, 1253, 1246, 1172, 1112, 1090, 1038, 9499, 801 and 749; δ_H (300 MHz; $CDCl_3$) 7.09 (2H, d, CH of Ar), 6.81 (2H, d, CH of Ar), 3.82 (1H, s, OCH_3), 3.54 (6H, q, CH_2CH_3), 2.37 (2H, quintet, $CH_2CH_2CH_2Si$), 1.21 (3H, t, CH_2CH_3) and 0.64 (2H, t, CH_2Si); δ_C (75.5 MHz; $CDCl_3$) 157.61 ($COCH_3$), 134.41 (CCH_2), 129.30 (s, CH of Ar), 113.55 (CH of Ar), 58.23 (OCH_2 CH_3), 55.12 (CH_3O), 38.20 (CH_2Ar), 24.95 (s, $CH_2CH_2CH_2Si$), 18.21 (CH_2CH_3) and 9.97 (CH_2Si); δ_{Si} (79.3 MHz; $CDCl_3$) −45.42; *m/z* (EI) 313 (M^+), 270, 256, 238, 227, 210, 196, 165, 121, 107, 91 and 77; Found: C, 61.53; H, 9.20%. $C_{16}H_{28}SiO_4$ requires C, 61.50; H, 9.20.

4.3.2. Octa-3-para-methoxyphenylpropyl-octasilsesquioxane **5**

3-*para*-Methoxyphenylpropyltriethoxysilane (1.11 g, 3.54 mmol) was dissolved in chloroform (50 cm^3) and TBAF *Solution A* (1.77 cm^3) added. The mixture was stirred at room temperature for 24 h then the mixture washed with water (3 × 50 cm^3). The organic layer was separated and a combination of white solid and yellow oil obtained after removal of the solvent. This residue was extracted with acetone (5 cm^3) to give a white solid after filtration. Crystals suitable for X-ray structure analysis were prepared by re-crystallising the solid from a 1:1 dichloromethane/acetone solution. Yield: 0.13 g (17%); m.p. 144 °C; ν_{max} (/cm^{-1}) 2730, 2671, 1610, 1580, 1513, 1305, 1253, 1194, 1150, 1023, 823, 771, 734 and 689; NMR: δ_H (300 MHz, $CDCl_3$) 0.55 (16H, t, $SiCH_2$), 1.78 (16H, m, $SiCH_2$ CH_2CH_2Ar), 2.47 (16H, t, CH_2Ar), 3.69 (24H, s, CH_3), 6.71 (16H, d, CH of Ar) and 6.93 (16H, d, CH of Ar); δ_C (75.5 MHz, $CDCl_3$) 12.30 ($SiCH_2$), 25.07 ($SiCH_2CH_2CH_2Ar$), 37.97 (CH_2Ar), 55.28 (CH_3), 113.76 (CH of Ar), 129.36 (CH of Ar), 134.50 (C of Ar) and 158.70 (C of Ar); δ_{Si} (79.3 MHz, $CDCl_3$) −66.77; *m/z* (MALDI-TOF): 1610.55 (100%, $[M + H]^+$).

4.3.3. Octa-iso-octyl-octasilsesquioxane **6**

Iso-octyltrimethoxysilane (0.58 g, 2.48 mmol) and TBAF *Solution A* (1.2 cm^3) were dissolved in dichloromethane (50 cm^3) and stirred for two days. The solution was extracted with water (20 cm^3) and further dichloromethane (200 cm^3) and the organic phase separated and dried over magnesium sulfate. The solvent was then removed under vacuum and the residue washed with acetone (20 cm^3) to give a colourless oil. The oil was purified by column chromatography (SiO_2/hexane) giving a single fraction of **6**. Yield: 0.18 g (43%); NMR: δ_H (300 MHz, $CDCl_3$) 0.58 (16H, d, $^1J_{HH}$ = 8.25 Hz, $SiCH_2$), 0.89 (72H, s, $C(CH_3)_3$), 1.00 (24H, d, $^1J_{HH}$ = 6.33 Hz, $CHCH_3$), 1.14 (16H, d, $^1J_{HH}$ = 6.42 Hz, $CH_2C(CH_3)_3$) and 1.30 (8H, m, CH); δ_C (300 MHz, $CDCl_3$) 12.36 ($SiCH_2$), 23.54 ($CHCH_3$), 24.97 ($CH_2C(CH_3)_3$), 30.13 ($C(CH_3)_3$), 30.93 (CH) and 53.90 ($C(CH_3)_3$); δ_{Si} (400 MHz, $CDCl_3$) −68.20; *m/z* (MALDI-TOF): 1323.42 $[M + H]^+$.

4.3.4. Octa-cyclopentyl-octasilsesquioxane **8**

This is a known compound and was first characterised by Barry et al. [18]. Therefore the experimental details presented here are only to demonstrate the various reaction and workup conditions that resulted in the crystals of the new solid state structures for this compound that we have obtained.

4.3.4.1. Octa-cyclopentyl-octasilsesquioxane crystal structure **8a**.

2 (0.04 g, 0.05 mmol), alkoxysilane (0.03 g, 0.16 mmol) and TBAF *Solution A* (0.03 cm^3) were dissolved in dichloromethane (20 cm^3) and stirred for 24 h. The solution was then extracted with water (10 cm^3) and further dichloromethane (100 cm^3) and the organic phase dried over magnesium sulfate. The solvent was then removed under vacuum and the residue washed

with acetone (20 cm^3) to give **8** as a white solid. The solid was recrystallised from a dichloromethane/acetone mixture to give colourless crystals of **8a** suitable for X-ray structure analysis.

*4.3.4.2. Octa-cyclopentyl-octasilsesquioxane crystal structure **8b**.* **2** (0.16 g, 0.19 mmol), alkoxysilane (0.10 g, 0.40 mmol) and TBAF *Solution A* (0.10 cm^3) were dissolved in dichloromethane (50 cm^3) and stirred for 24 h. The solution was then extracted with water (20 cm^3) and dichloromethane (200 cm^3) and the organic phase dried over magnesium sulfate. The solvent was then removed under vacuum and the residue washed with acetone (20 cm^3) to give a colourless gel. Crystals of **8b** suitable for X-ray structure analysis were prepared by crystallising the material from a 1:1 dichloromethane/acetone solution.

*4.3.4.3. Octa-cyclopentyl-octasilsesquioxane crystal structure **8c**.* **2** (0.20 g, 0.25 mmol), alkoxysilane (0.12 g, 1.02 mmol) and TBAF *Solution A* (0.13 cm^3) were dissolved in dichloromethane (50 cm^3) and stirred for 24 h. The solution was then extracted with water (20 cm^3) and dichloromethane (200 cm^3) and the organic layer dried over magnesium sulfate. The solvent was then removed under vacuum leaving a residue containing predominantly **8**. Following ^{29}Si NMR analysis of this residue dissolved in deuteriochloroform, crystals of **8c** suitable for X-ray crystal structure analysis were formed inside the NMR tube and were separated by decanting the solution.

4.4. ^{18}O labelling experiments

4.4.1. Reaction (a)

Cyclopentyltriethoxysilane (0.089 g/0.38 mmol) was dissolved in dry acetone (2 cm^3) and TBAF *Solution A* (100 μl) added. The mixture was stirred to give a white solid product of **7** which precipitated from solution after 30 min and was characterised from its FTICR mass spectrum.

4.4.2. Reaction (b)

Cyclopentyltriethoxysilane (0.087 g/0.37 mmol) was dissolved in dry acetone (2 cm^3) and TBAF *Solution C* (188 μl) added. The mixture was stirred to give a white solid product of **7** which precipitated from solution after 30 min and was characterised from its FTICR mass spectrum.

4.4.3. Reaction (c)

Cyclopentyltriethoxysilane (0.089 g/0.38 mmol) was dissolved in dry acetone (2 cm^3) and TBAF *Solution D* (100 μl) added. The mixture was stirred to give a white solid product of **7** which precipitated from solution after 30 min and was characterised from its FTICR mass spectrum.

4.4.4. Reaction (d)

Cyclopentyltriethoxysilane (0.092 g/0.40 mmol) was dissolved in dry acetone (2 cm^3) and TBAF *Solution A* (100 μl) added. The mixture was stirred to give a white solid product of **7** which precipitated from solution after 30 min and was characterised from its FTICR mass spectrum.

4.4.5. Reaction (e)

Cyclopentyltriethoxysilane (0.090 g/0.39 mmol) was dissolved in dry acetone (2 cm^3) and TBAF *Solution D* (100 μl) added. The mixture was stirred to give a white solid product of **7** which precipitated from solution after 30 min and was characterised from its FTICR mass spectrum.

4.4.6. Reaction (f)

Cyclohexyltriethoxysilane (0.096 g/0.39 mmol) was dissolved in dry acetone (2 cm^3) and TBAF *Solution A* (100 μl) added. The mixture was stirred to give a white solid product of **7** which precipitated from solution after 30 min and was characterised from its FTICR mass spectrum.

4.4.7. Reaction (g)

Cyclohexyltriethoxysilane (0.099 g/0.40 mmol) was dissolved in dry acetone (2 cm^3) and TBAF *Solution D* (100 μl) added. The mixture was stirred to give a white solid product of **7** which precipitated from solution after 30 min and was characterised from its FTICR mass spectrum.

4.5. Preparation of disiloxanes from monochlorosilanes by hydrolysis using the water contained in a TBAF solution

The siloxanes prepared are known compounds and characterised only from the EI mass spectra of species of interest immediately following GC separation.

4.5.1. Hydrolysis of (chloro)methyldiphenylsilane

(Chloro)methyldiphenylsilane (0.13 g/0.52 mmol) was dissolved in dry acetone (2 cm^3) and after TBAF *Solution D* (200 μl) was added the solution was stirred for 24 h. The solvent was then removed under vacuum and the remaining oily residue characterised without further purification. Isolated:

a: 1,3-Dimethyl-1,1,3,3-tetraphenyldisiloxane: m/z (EI): 397 (100%, $[M_{O18} - Me]^+$), 395 (34%, $[M_{O16} - Me]^+$), 319 (64%, $[M_{O18} - Me - Ph]^+$), 317 (23%, $[M_{O16} - Me - Ph]^+$).

b: 1-Fluoro-1,3-dimethyl-1,3,3-triphenyldisiloxane: m/z (EI): 339 (100%, $[M_{O18} - Me]^+$), 337 (65%, $[M_{O16} -$

Table 5
Crystal data, data collection and refinement parameters for compounds **5**, **8a**, **8b**, **8c** and **10**

	5	**8a**	**8b**	**8c**	**10**
Formula	$C_{80}H_{104}O_{20}Si_8$	$C_{48}H_{88}O_{12}Si_8$	$C_{48}H_{88}O_{12}Si_8$	$C_{48}H_{88}O_{12}Si_8$	$C_{64}H_{136}O_{12}Si_8$
Molecular weight	1610.35	1081.90	1081.90	1081.90	1322.45
Colour	Colourless	Colourless	Colourless	Colourless	Colourless
Morphology	Plate	Block	Block	Block	Plate
Crystal size (mm)	$0.07 \times 0.05 \times 0.02$	$0.25 \times 0.20 \times 0.15$	$0.25 \times 0.20 \times 0.15$	$0.20 \times 0.20 \times 0.15$	$0.20 \times 0.20 \times 0.15$
Crystal system	Triclinic	Rhombohedral	Triclinic	Tetragonal	Triclinic
Space group	$P\bar{1}$	$R\bar{3}$	$P\bar{1}$	$P4/n$	$P\bar{1}$
Unit cell dimensions					
a (Å)	9.2155(2)	16.6048(8)	17.0886(8)	15.7365(2)	8.5186(4)
b (Å)	20.0378(4)	16.6048(8)	17.8454(8)	15.7365(2)	9.1418(4)
c (Å)	22.6830(5)	17.3069(7)	25.4512(15)	12.5643(4)	25.8700(13)
α (°)	81.137(2)	90	77.133(2)	90	80.073(2)
β (°)	83.650(2)	90	71.658(2)	90	82.611(2)
γ (°)	81.934(2)	120	88.819(2)	90	84.185(3)
V (Å^3)	4080.66(15)	4132.57(13)	7171.85(16)	3111.39(11)	1961.52(16)
Z	2	3	5	2	1
D_{calc} (g cm^3)	1.311	1.304	1.252	1.155	1.120
$F(0\,0\,0)$	1712	1752	2920	1168	728
Temperature (K)	150(2)	120(2)	120(2)	120(2)	120(2)
Reflections collected	25 601	9148	72 647	15 246	15 392
Independent reflections	12 287	1631	22 578	2737	6614
R_{int}	0.0764	0.1264	0.3726	0.0611	0.0733
θ Range (°)	2.95–23.75	3.07–25.02	2.99–25.03	3.05–25.02	2.99–25.03
h Range	−9, 10	−19, 15	−20, 20	−18, 18	−9, 10
k Range	−20, 22	−16, 19	−20, 21	−18, 18	−10, 10
l Range	−25, 25	−19, 20	−27, 28	−11, 14	−30, 30
Final R indices [$F^2 > 2\sigma(F^2)$]	$R_1 = 0.0978$, $wR_2 = 0.1750$	$R_1 = 0.1217$, $wR_2 = 0.3100$	$R_1 = 0.1680$, $wR_2 = 0.3719$	$R_1 = 0.0553$, $wR_2 = 0.1653$	$R_1 = 0.0705$, $wR_2 = 0.1792$
R indices (all data)	$R_1 = 0.2173$, $wR_2 = 0.2006$	$R_1 = 0.2528$, $wR_2 = 0.3948$	$R_1 = 0.4744$, $wR_2 = 0.4975$	$R_1 = 0.0553$, $wR_2 = 0.1653$	$R_1 = 0.1468$, $wR_2 = 0.2230$
S (goodness-of-fit on F^2)	1.165	1.111	1.046	0.793	0.955
N_{ref}	12 287	1631	22 578	2737	6614
N_{par}	900	118	1531	154	419

Me]$^+$), 261 (38%, [M_{O18} − Me − Ph]$^+$), 259 (23%, [M_{O16} − Me − Ph]$^+$).

4.5.2. Hydrolysis of chlorotrimethylsilane

Chlorotrimethylsilane (0.05 g/0.46 mmol) was dissolved in dry acetone (2 cm^3) and after TBAF *Solution D* (200 μl) was added the solution was stirred for 24 h. The solvent was then removed under vacuum and the remaining oily residue characterised without further purification. Isolated:

Hexamethyldisiloxane: m/z (EI): 149 (100%, [M_{O18} − Me]$^+$), 147 (49%, [M_{O16} − Me]$^+$).

4.6. Synthesis of 7 under 'dry' and 'wet' TBAF conditions

4.6.1. 'Dry' conditions

Cyclopentyltriethoxysilane (0.05 g/0.19 mmol) was dissolved in deuterioacetone (1.5 cm^3) in a septa-sealed NMR tube and TBAF *Solution B* (50 μl) added. The mixture was briefly shaken, allowed to stand for 24 h and then analysed by ^{29}Si NMR spectroscopy. The significant chemical shift results are reported in Section 2.

4.6.2. 'Wet' conditions

The reaction was performed in the same manner and with the same analysis method as for the 'dry' reaction but using TBAF *Solution A* (50 μl) supplemented by water (100 μl). The significant chemical shift results are reported in Section 2.

4.7. Synthesis of 7 using TBAF in different solvents

These reactions were carried out by the standard method [12] using TBAF *Solution A* and the appropriate solvent (30 cm^3).

4.8. X-ray crystallography

All structures were measured on a Nonius Kappa CCD diffractometer (ϕ scans and ω scans to fill *asymmetric unit* or *Ewald* sphere) using graphite monochromated Mo Kα radiation ($\lambda = 0.71073$ Å). The data collection was performed in a ψ rotation mode. A list of crystal data, data collection, structure solution and refinement parameters is provided in Table 5. The raw intensity data was corrected for Lorentz and polarisation effects as well as absorption correction (SORTAV) [27]. Structure solutions were searched and refined by Direct Methods [28] (SHELXS 97) and Difference Fourier Analyses (SHELXL 97) [29], respectively, based on F^2. Atom form factors for neutral atoms were taken from the literature [30]. Second and third row elements were allowed to refine anisotropically with hydrogen atoms assumed in idealised positions riding on their pivot atoms.

5. Supplementary data

Crystallographic data for the structures reported in this paper has been deposited with the Cambridge Crystallographic Data Centre as Supplementary Publication Nos. CCDC 216990–216994. Copies of the data can be obtained free of charge on application to CCDC, 12 Union Road, Cambridge, CB2 1EZ, UK, fax: (+44) 1223 336 033. Email: data_request@ccdc.cam.ac.uk.

Acknowledgement

We thank Dow Corning for their support of Y.Y.

References

[1] I.M. Saez, J.W. Goodby, Liquid Cryst. 26 (1999) 1101.
[2] R. Elsaber, G.H. Mehl, J.W. Goodby, D.J. Photinos, J. Chem. Soc., Chem. Commun. (2000) 851.
[3] F.J. Feher, K.D. Wydham, M.A. Sciadone, Y. Hamuro, J. Chem. Soc., Chem. Commun. (1998) 1469.
[4] F.J. Feher, J. Am. Chem. Soc. 108 (1986) 3850.
[5] F.J. Feher, R.L. Blanski, J. Chem. Soc., Chem. Commun. (1990) 1614.
[6] F.J. Feher, K.D. Wyndham, J. Chem. Soc., Chem. Commun. (1998) 323.
[7] A.R. Bassindale, T.E. Gentle, J. Mater. Chem. 12 (1993) 1319.
[8] P.A. Agaskar, Inorg. Chem. 30 (1991) 2707.
[9] J.F. Brown, L.H. Vogt, J. Am. Chem. Soc. 87 (1965) 4313.
[10] H. Behbehani, B.J. Brisdon, M.F. Mahon, K.C. Molloy, J. Organometal. Chem. 469 (1994) 19.
[11] F.J. Feher, D.A. Newman, J.F. Walzer, J. Am. Chem. Soc. 111 (1989) 174.
[12] A.R. Bassindale, Z. Liu, I.A. MacKinnon, P.G. Taylor, Y. Yang, M.E. Light, P.N. Horton, M.B. Hursthouse, J. Chem. Soc., Dalton Trans. (2003) 2945.
[13] A.R. Bassindale, Z. Liu, D.J. Parker, P.G. Taylor, P.N. Horton, M.B. Hursthouse, M.E. Light, J. Organometal. Chem. 687 (2003) 1.
[14] R. Maurer, F.H. Kreuzer, P. Spes, Makromol. Chem. Macromol. Symp. 30 (1991) 215.
[15] J.W. Goodby, G.H. Mehl, Chem. Ber. 129 (1996) 521.
[16] G.H. Mehl, J.W. Goodby, Angew. Chem., Int. Ed. Engl. 35 (1996) 2641.
[17] G.H. Mehl, J.W. Goodby, I.M. Saez, R.P. Tuffin, G.H. Mackenzie, R. Auzely-Velty, T. Benvegru, D. Plusquellec, J. Chem. Soc., Chem. Commun. (1998) 2057.
[18] A.J. Barry, W.H. Daudt, J.J. Domicons, J.W. Gilkey, J. Am. Chem. Soc. 77 (1955) 4248.
[19] N.V. Podberezskaya, I.A. Baidina, V.I. Alekseev, S.V. Borisov, T.N. Martynova, J. Struct. Chem. (Engl. Transl.) 22 (1981) 737.
[20] P.-A. Jaffrès, R.E. Morris, J. Chem. Soc., Dalton Trans. (1998) 2767.
[21] C. Bonhomme, P. Toledano, J. Maquet, J. Livage, L. Bonhomme-Coury, J. Chem. Soc., Dalton Trans. (1997) 1617.
[22] I. Richter, C. Burschka, R. Tacke, J. Organomet. Chem. 646 (2002) 200.
[23] U. Dittmar, B.J. Hendan, U. Flörke, H.C. Marsmann, J. Organomet. Chem. 489 (1995) 185.
[24] F.J. Feher, T.A. Budzichowski, J. Organomet. Chem. 373 (1989) 153.

[25] N.V. Podberezskaya, S.A. Magarill, I.A. Baidina, S.V. Borisov, L.É. Gorsh, A.N. Kanev, T.N. Martynova, J. Struct. Chem. (Engl. Transl.) 23 (1982) 422.
[26] M.A. Hossain, M.B. Hursthouse, K.M.A. Malik, Acta Crystallogr. B35 (1979) 2258.
[27] (a) R.H. Blessing, Acta Crystallogr. A51 (1995) 33;
(b) R.H. Blessing, J. Appl. Crystallogr. 30 (1997) 421.
[28] G.M. Sheldrick, SHELXS 97_2. A Program for Crystal Structure Solution, University of Göttingen, FRG, 1998.
[29] G.M. Sheldrick, SHELXL 97_2. A Program for Crystal Structure Refinement, University of Göttingen, FRG, 1998.
[30] International Tables for Crystallography, vol. C, Tables 4.2.6.8 and 6.1.1.4, Kluwer Academic Publishers, Dordrecht, The Netherlands, 1995.